

Composite Membranes Based on SBA – 15 and SBA – 16 Evaluated at High Temperature and Low Relative Humidity Fuel Cell Conditions

C. Guzmán¹, A. Alvarez¹, J. Ledesma-García², S.M. Duron – Torres³, L.G. Arriaga^{1,*}

¹ Centro de Investigación y Desarrollo Tecnológico en Electroquímica S.C., C.P. 76703, Querétaro, México.

² División de Investigación y Posgrado, Facultad de Ingeniería, Universidad Autónoma de Querétaro, C.P. 76010, Querétaro, México.

³ UACQ – UAZ, CU Siglo XXI Edificio b, Km 6 Carr. Zac – Gdl, La Escondida Zacatecas, Zac, C.P. 96160, México.

*E-mail: lariaga@cideteq.mx

Received: 5 July 2011 / Accepted: 12 September 2011 / Published: 1 October 2011

Composite membranes containing mesoporous materials (SBA – 15 and SBA – 16) were tested under high temperature (140 °C) and low relative humidity (22.9 %) fuel cell operating conditions. SBA – 15 and 16 membranes showed better performance at high temperature (140 °C) and low relative humidity (22.9 %) than a commercial Nafion Membrane. SBA – 16 showed better performance (0.13 W cm⁻²) at high temperature (140 °C) and low relative humidity (22.9 %) than the SBA – 15 membrane (0.015 W cm⁻²). Cycle testing (1000 cycles) showed that the SBA – 15 membrane was more stable than the SBA – 16 membrane under extreme operating conditions (22.9 % RH and 120 °C). We suggest that this improvement is related to the water retention of the inorganic fillers due to the dipole - dipole interactions between water and the fillers. These new membranes are good candidates to replace commercial Nafion membranes.

Keywords: High temperature fuel cells, low relative humidity, SBA – 15, SBA – 16.

1. INTRODUCTION

Proton exchange fuel cells (PEMFCs) have been considered excellent candidates to replace the conventional technologies used to generate electricity. PEMFCs are typically operated between 60 – 80 °C with pure H₂ and O₂ [1-5]. Nafion membranes exhibit excellent performance at 80 °C and high humidity conditions; under these conditions, the maximum conductivity occurs at approximately 0.083 Scm⁻¹ [6]. All of these characteristics indicate optimum performance.

Increasing the operating temperature to above 80 °C can improve the electrode kinetics related to the oxygen reduction reaction, resulting in high performance and an increase in CO tolerance [7, 8]; however, at high temperatures, the conductivity of Nafion decreases drastically due to membrane dehydration, elevating the ohmic resistance [9, 10].

Another problem is the water vapor in the stream gases. At high temperatures, larger amounts of water vapor are required to maintain a given amount of water in the membrane. If a fuel cell is to use oxygen from air, the total oxygen content is approximately 21 % from the total stream, which is very small and, with humidification, decreases quickly with increasing temperature, producing lower cell voltages and weaker performance [11]. Figure 1 shows that with increasing temperature, the amount of water vapor increases and the O₂ and H₂ contents decrease in the stream. To compensate for this effect, it is necessary to raise the pressure of the gas stream, which is not possible in this type of fuel cell.

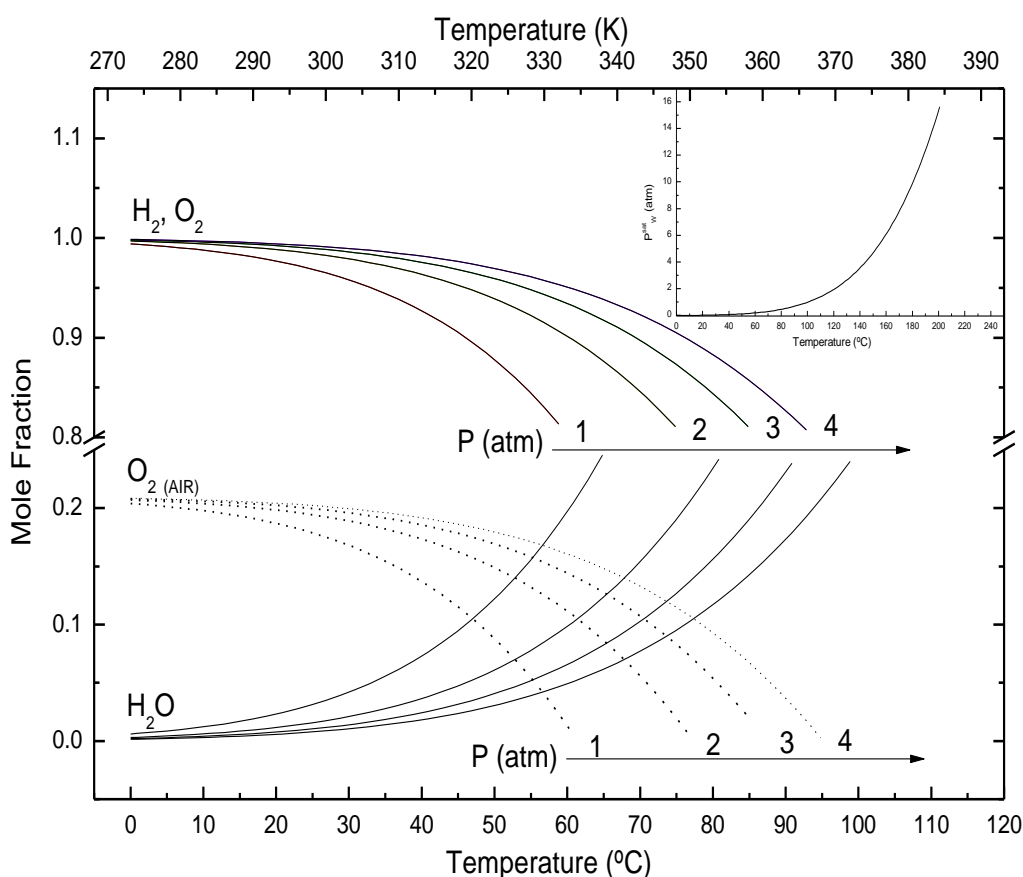


Figure 1. Show how the mole fractions of the reactants are dependent on pressure and temperature in fully humidified conditions. Inset shows the saturated vapor pressure of water.

Many researchers have reported that the addition of hydrophilic inorganic materials to the Nafion matrix can improve the mechanical properties, water retention and proton conductivity under high-temperature conditions (130 °C). Adjemian, Yang and Shao [8, 10, 12] observed that composite

membranes (SiO_2 , ZrO_2 and ZrO_2 – PWA respectively) can retain water at high temperature and low humidification levels (70 %). Saccà [13] reported better performance using 10 % (w/w) ZrO_2 in Nafion at 130 °C and 80 % RH.

Recent studies [14-16] have reported the advantages of use mesoporous silica in Nafion matrices; this organized silica enhances the proton conductivity at high temperatures of up to 100 °C and lower relative humidity (10%); this improvement is related to the aligned mesoporous channels in the silica. In a previous study [17], we observed good stability using mesoporous silica (SBA – 15) under high relative humidity (70%) and high temperature. These types of materials have not been tested under low relative humidity (22.9 %) and high temperature (140 °C). The aim of the present work was to incorporate mesoporous materials (SBA – 15 and 16) synthesized via sol-gel processing into a Nafion matrix to take advantage of the conductivity improvements at high temperature (140 °C) and low relative humidity (22.9 %) in a hydrogen/oxygen PEM fuel cell and observe the stability of the membrane by cycling under low relative humidity (22.9 %) and high temperature (120 °C).

2. EXPERIMENTAL

2.1. Synthesis of the inorganic fillers

SBA – 15 was synthesized using Pluronic P123 triblock copolymer as a surfactant structure and directing agent. It was dissolved in a solution of 4M HCl under stirring conditions. TEOS was added to the solution at room temperature (35 °C) for 24 h. The resulting slurry was heated at 80 °C for 24 h. The resulting product was washed with deionized water and filtered. Then it was dried with air at room temperature of 110 °C for 18 h. Finally, it was heated at 500 °C for 6h in order to remove the organic template.

SBA – 16 was synthesized using P 127 as a surfactant and structure directing agent. TEOS was added drop by drop into a 2 M HCl solution and stirred at room temperature for 24 h. The resulting slurry was heated at 80 °C for 48 h. The resulting product was washed with deionised water and filtered. Then it was dried with air at room temperature of 110 °C for 18 h. Finally, it was heated at 500 °C for 6h in order to remove the organic template.

2.2. Membrane Preparation and Physico – chemical Characterization

Composite membranes containing 5% Nafion solution (Electrochem 5% in alcohol) and 3 wt. % inorganic fillers were prepared using a combination of recast and heat treatment procedures that are described elsewhere [18]. A subsequent chemical cleaning treatment was performed using a previously reported method [19] that consists of (i) boiling in 3% hydrogen peroxide for 1 h and then rinsing with water, (ii) boiling in 0.5 M sulfuric acid for 1 h and then rinsing with water and (iii) boiling in a water bath for 1 h to remove any excess acid. The morphology of the composite membranes was observed by scanning electron microscopy (SEM) in a JEOL JSM-6060 LV microscope, and surface mapping was conducted by energy dispersive X-ray spectroscopy (EDXS).

2.3. Fuel cell Evaluation

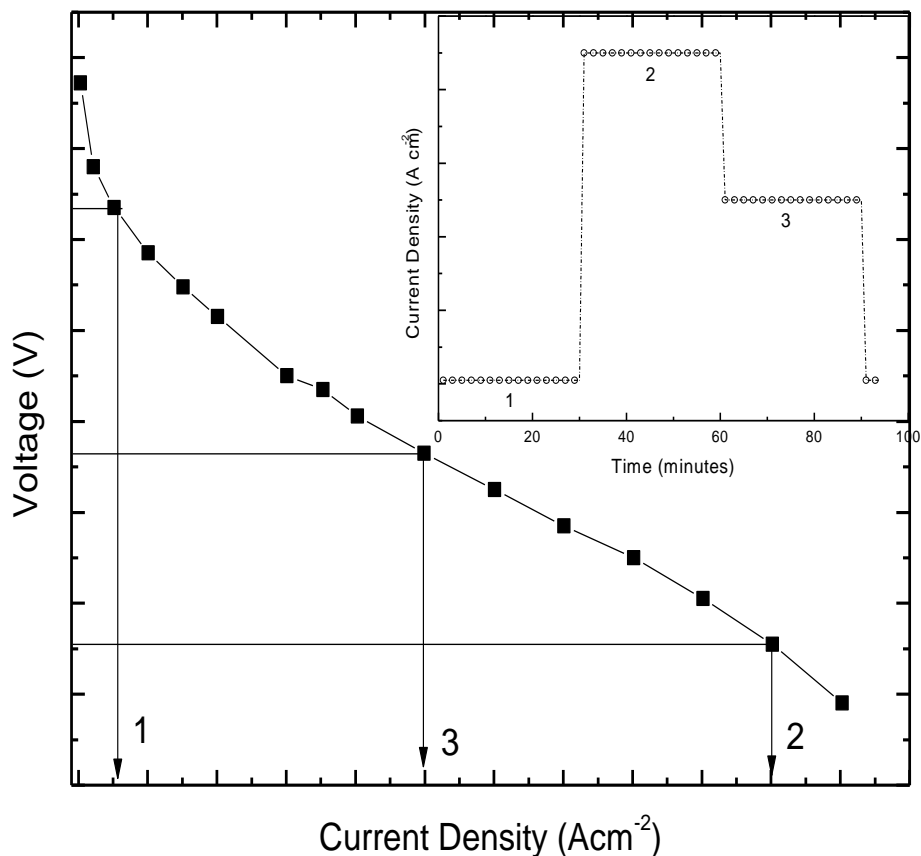


Figure 2. (a) Low, medium and High current points and (b) Schematic Complete Current aging cycle.

Table 1. Experimental conditions of the fuel cell system.

Cell Temperature (°C)	Back Pressure (psi)	Relative Humidity (% RH)	Gases Stoichiometry	
			H ₂	O ₂
80	30	100	1.5	2
	30	22.9	1.5	2
100	30	22.9	1.5	2
120	30	22.9	1.5	2
140	30	22.9	1.5	2

The electrocatalytic deposit was made via a spray method by Ion Power Inc. with a platinum loading of 0.3 mg Pt/C 30% E – Tek on the composite membranes. We used a high-temperature carbon cloth with teflon as gas diffusion layers (Ion Power Inc.). The performance test was performed on a single 5-cm² (Electrochem) cell connected to an Electrochem PS - CompuCell fuel cell test station. The experimental conditions are shown in table 1.

Cyclic current aging was performed. Each current aging cycle is illustrated in Figure 2. It was composed of three current steps (Nafion = 0.25, 1 and 2 A; composite membranes = 0.25, 1, 3.5 A) in which the voltage was a function of the cycle number. A degradation test was performed at $T_{\text{Cell}} = 120$ °C, 30 psi of back pressure and 22.99 % relative humidity.

3. RESULTS

Figure 3 shows the morphology of the inorganic fillers obtained. The SBA – 15 presented a homogenous cylinder morphology, while in SBA – 16 the particles presented a spherical uniform shape.

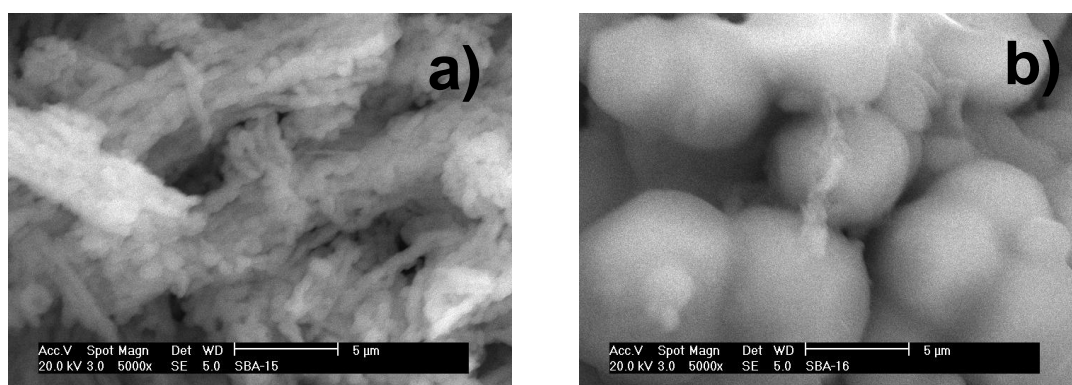


Figure 3. SEM images of the inorganic fillers a) SBA – 15 and b) SBA – 16.

The surface area obtained previously [17, 20] by BET, was of 932 and 625 m² g⁻¹ respectively, the high surface area is expected to have a contribution in the performance due to the water retention in this materials via dipole – dipole interactions between the water and the inorganic material.

Figure 4 shows SEM images and their corresponding elemental analysis for Si and F for the surface of the composite membranes. Nafion morphology and elemental analysis are shown in figure 4 a. As we expected a high concentration of F was obtained from the structure of Nafion (Figure 4 a ii). SBA – 15 morphology and its corresponding elemental analysis indicates that the dispersion of the inorganic filler is homogenous (Figure 4b). The mapping showed a high concentration of F (Figure 4b ii) attributed to the Nafion structure. Silicon (Figure 4b iii) distribution is homogeneous and covers all the measured area of the membrane with a good dispersion. SBA – 16 (figure 4 c) presents an agglomeration of the material on the surface, the mapping of Si (Figure 4 c iii) showed an agglomeration of the material on the membrane.

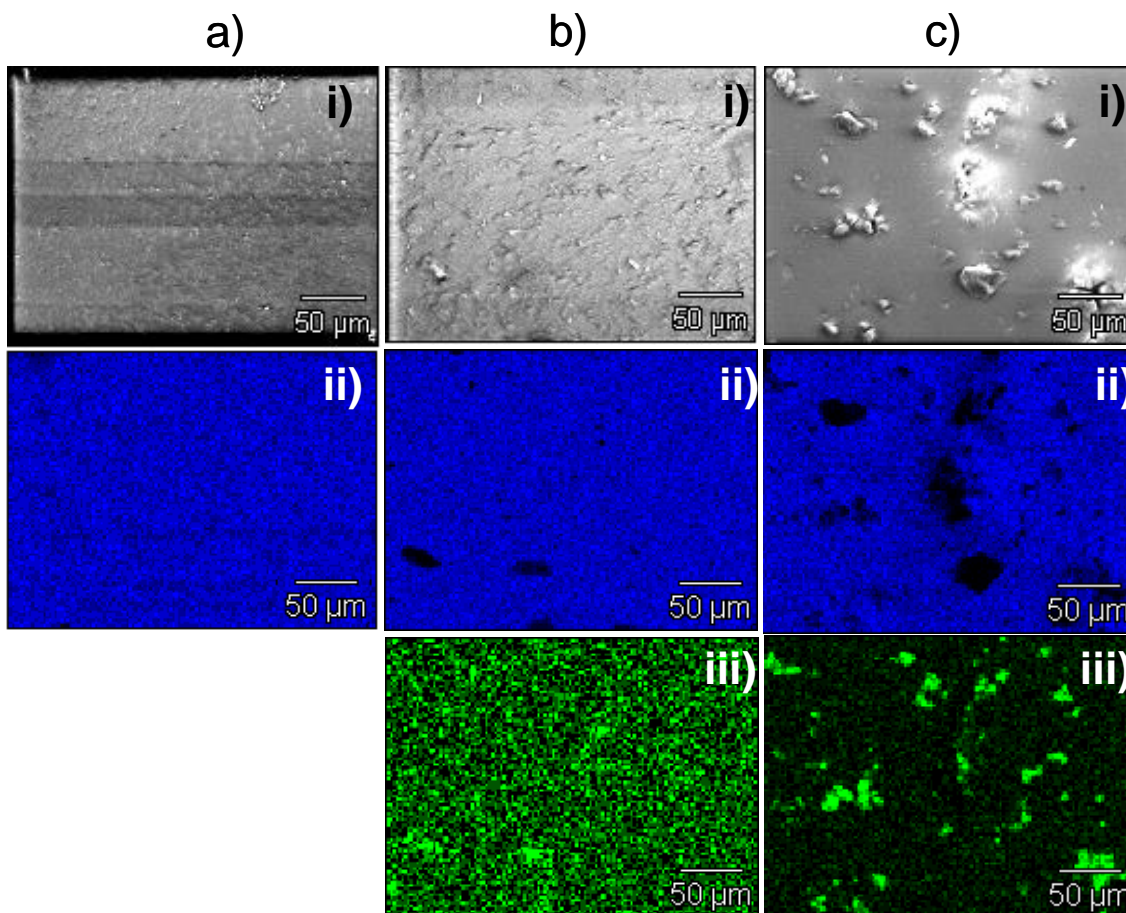


Figure 4. SEM images with a elemental mapping of (II) Fluoride and (III) Silicon for a) Nafion, b) SBA - 15 and c) SBA – 16 at 1000X.

Table 2. Experimental parameter from the composite membranes.

Membrane	R ($\Omega \text{ cm}^{-2}$)				E_{OCV} (V)				W_{Max} (W cm^{-2})			
	80	100	120	140	80	100	120	140	80	100	120	140
Nafion	0.31	0.36	0.42	1.42	0.99	0.93	0.93	0.92	0.27	0.28	0.15	0.009
SBA - 15	0.38	0.42	0.2	1.52	0.93	0.9	0.92	0.9	0.16	0.21	0.14	0.015
SBA – 16	0.22	0.28	0.48	1.25	1.01	0.99	0.97	0.94	0.54	0.31	0.25	0.13

Figure 5 shows the polarization curves of the composite membranes (SBA – 15 and 16) compared to a commercial Nafion 115 membrane (Nafion E – Tek 0.3 mg Pt/C) under fully hydrated conditions (100 % RH) at 80 °C. The SBA – 16 membrane shows the highest performance (0.52 W cm^{-2}) compared to the Nafion (0.35 W cm^{-2}) and SBA – 15 (0.17 W cm^{-2}) membranes. This improvement in the performance on the SBA -16 membrane is related to water retention in the inorganic filler, a testament to the filler’s hygroscopic properties. The low performance on the SBA –

15 is related with the high values of resistance obtained due to the presence of the inorganic material with high superficial area.

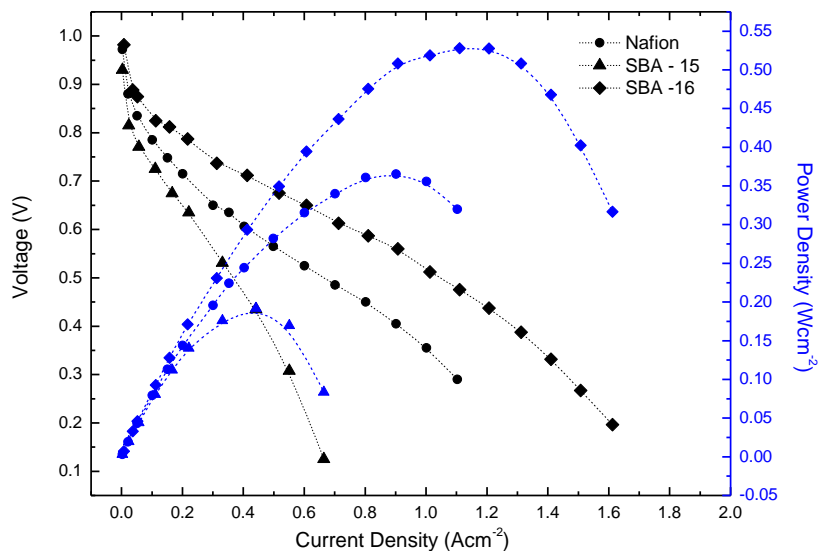
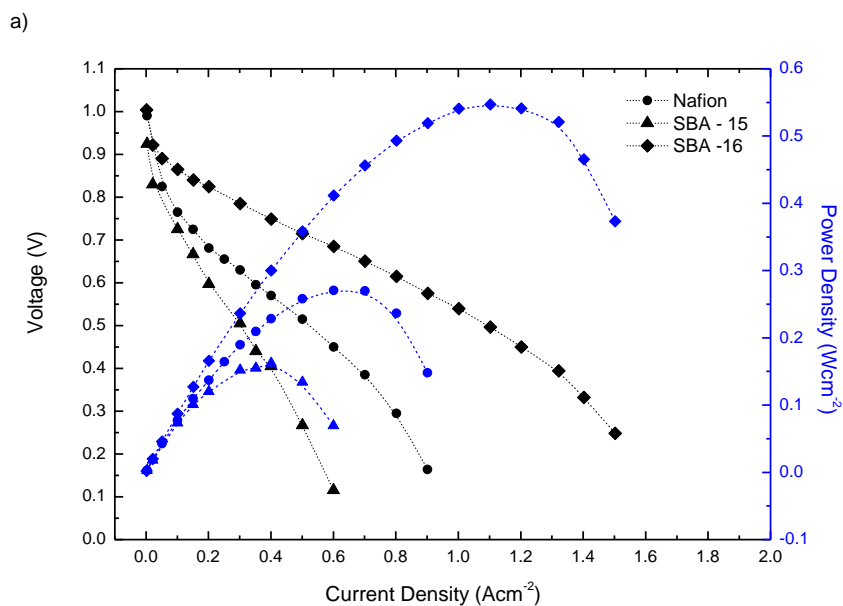


Figure 5. Polarization curves of the composite membranes at $T_{cell} = 80\text{ }^{\circ}\text{C}$ and 100% of relative humidity.

Decreasing the relative humidity to 22.9 % (Figure 5 a), SBA – 16 membrane adopts a behavior similar to that observed at 100% RH; this suggests that the MEA is independent of the relative humidity (Figure 6 a).



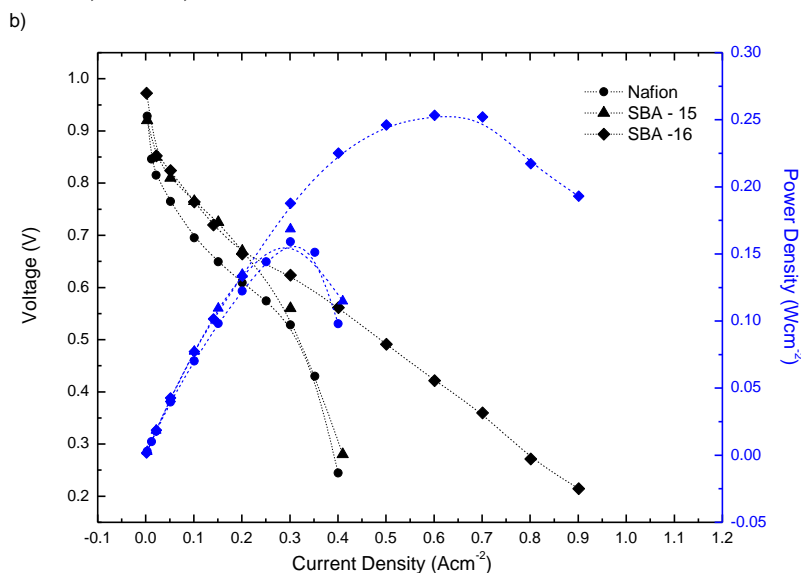
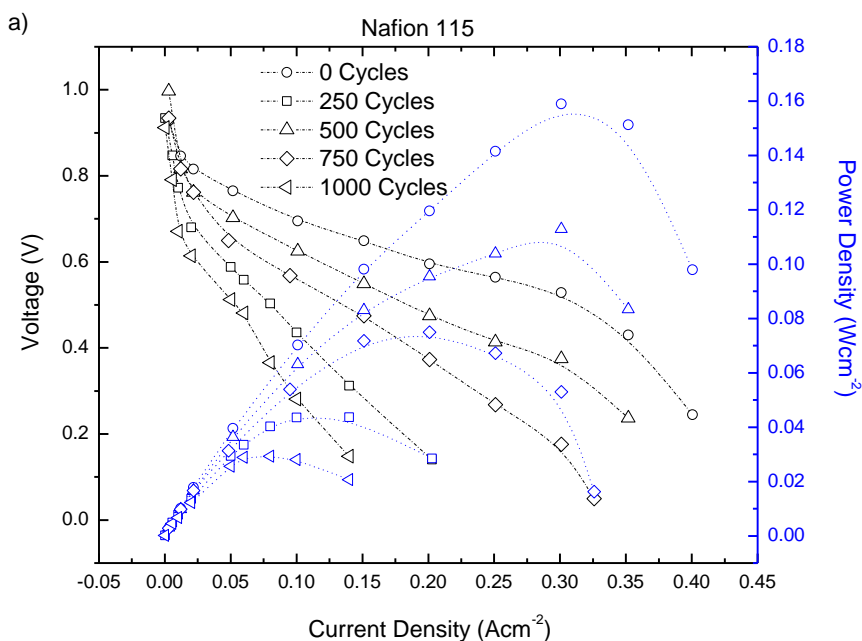


Figure 6. Polarization Curves of the composite membranes at 22.9 % of relative humidity and temperature of a) 80, b) 120 °C.

The polarization curves at 22.9 % relative humidity were performed after 30 minutes of stabilization at this temperature. With the increase in temperature, the power density and cell resistance decrease due to membrane dehydration. SBA – 16 has the highest power density values and the smallest cell resistance values across the whole range of temperatures tested (Table 2). When the temperature reached 120 °C (Figure 6 b), SBA – 16 maintained its maximum performance, but the SBA – 15 exhibited the same level of performance as the Nafion membrane. The resistance values of the SBA – 15 membrane are higher over the entire temperature range; this could be the reason for its weak observed performance. Above 120 °C, the inorganic fillers facilitated water transport. In previous work [21], the water transport was reported to be better than in Nafion due to dipole – dipole interactions between the water molecules and the inorganic fillers, maintaining the membrane hydrated.



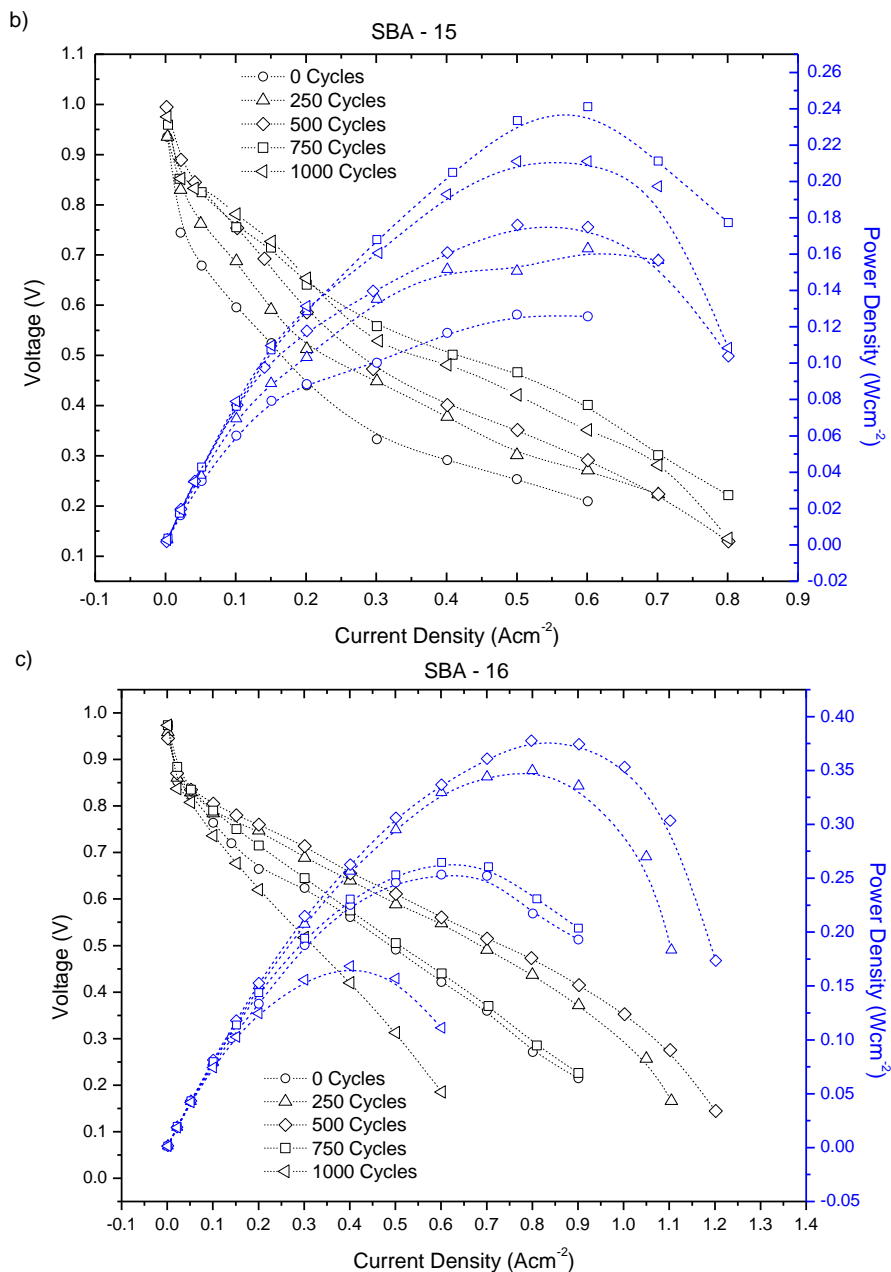


Figure 7. Polarization curves every 250 cycles at $T_{cell} = 120\text{ }^{\circ}\text{C}$ and 22.9% of relative humidity for a) Nafion, b) SBA – 15, c) SBA – 16

Table 3. Experimental parameter from the composite membranes.

Membrane	Nafion			SBA - 16			SBA – 15		
	Cycle	R	OCV	W_{Max}	R	OCV	W_{Max}	R	OCV
0	0.384	0.928	0.16	0.446	0.972	0.252	0.197	0.935	0.127
250	0.412	0.997	0.09	0.964	0.958	0.349	0.309	0.936	0.162
500	0.466	0.934	0.067	1.672	0.945	0.379	0.373	0.954	0.179
750	0.626	0.934	0.04	0.843	0.973	0.263	0.316	0.975	0.212
1000	1.241	0.912	0.029	1.987	0.973	0.171	0.373	0.995	0.241

Current cyclic aging was performed at 120 °C and 22.9 % relative humidity. The performance of the Nafion membrane decreased with the number of cycles, obtaining a final power density of 0.029 W cm⁻² six times less than the initial value. For the SBA – 15 membrane (Figure 7 b), the power density increased with the number of cycles, reaching a power density of 0.24 W cm⁻². The SBA – 16 membrane (Figure 7 c) showed similar behavior. The difference was that the durability of the MEA was approximately 1000 cycles, after which the power density was reduced to 0.171 W cm⁻², almost 50 % of the maximum power density value. The resistance and open-circuit voltage values are summarized in Table 3.

The high performance in the composite membranes after the aging cycle, at high temperatures and low RH conditions is related with the interactions of the inorganic filler and the water molecules into the Nafion matrix. The performance in Nafion occurs as a function of the water content inside of the membrane. In regions with a low water concentration, the proton is transported via diffusion with water molecules through a structure of low porosity (low water content $\lambda < 14$) [22].

However, with the incorporation of inorganic fillers, the porosity increases improving the water content into the Nafion matrix ($\lambda \approx 14$), according to Aricò and coworkers [23], SiO₂ forms Si–OH interactions. OH groups facilitates the water coordination acting as a water molecules trapping and vehicle molecule for proton migration. The water retained into the Nafion matrix helps to the transport of the proton increasing the water content into the membrane and improving the performance.

The experimental results show that composite membranes based on SBA – 15 and 16 improve the performance of a fuel cell at low relative humidity (22.9%) and high temperature (120 °C). This improvement is due to the addition of the inorganic oxide and the Nafion matrix, which provide better hydration of the membrane at reduced relative humidity; SBA – 15 and SBA – 16 were less susceptible to high-temperature damage due to membrane dehydration. Dehydration of the Nafion membrane at elevated temperatures leads to the destruction of the pore structure and decreases proton conductivity.

The silicon oxide prevented these temperature-based structural changes, maintaining proton conductivity [7]. SBA – 15 exhibits better stability than SBA – 16, which is related to the capacity of the former to retain water in the Nafion matrix. Improvement in proton transfer from the anode to the cathode was reflected by the performance at high temperatures (120 °C) and low relative humidity (22.9 %). These kinds of membranes are a promising alternative material for high-temperature PEMFC applications.

4. CONCLUSIONS

In this study, composite membranes showed good performance and stability compared to a commercial Nafion membrane. SBA – 16 exhibited good behavior in fuel cell tests but low stability compared to an SBA – 15 membrane. This phenomenon is attributed to the enhanced morphology and superficial area of the SBA – 15 membrane. The aim of this work was to validate these membranes as viable alternative materials to enable PEMFCs to operate at high temperatures and low relative humidity that simulate actual operating conditions.

ACKNOWLEDGMENTS

C. Guzmán and A. Alvarez The authors thanks to Mexican National Council of Science and Technology for the financial support SEP-CONACYT 133310, Fomix Zacatecas 81728.

References

1. L. Barelli, G. Bidini, F. Gallorini and A. Ottaviano, *International Journal of Hydrogen Energy*, In Press, Corrected Proof
2. V. Mishra, F. Yang and R. Pitchumani, *Journal of Power Sources*, 141 (2005) 47-64.
3. D. Seo, J. Lee, S. Park, J. Rhee, S. W. Choi and Y.-G. Shul, *International Journal of Hydrogen Energy*, In Press, Corrected Proof
4. M. V. Williams, H. R. Kunz and J. M. Fenton, *Journal of Power Sources*, 135 (2004) 122-134.
5. J. Zhang, Y. Tang, C. Song, X. Cheng, J. Zhang and H. Wang, *Electrochimica Acta*, 52 (2007) 5095-5101.
6. G. Alberti, M. Casciola, L. Massinelli and B. Bauer, *Journal of Membrane Science*, 185 (2001) 73-81.
7. K. T. Adjemian, S. J. Lee, S. Srinivasan, J. Benziger and A. B. Bocarsly, *Journal of The Electrochemical Society*, 149 (2002) A256-A261.
8. K. T. Adjemian, S. Srinivasan, J. Benziger and A. B. Bocarsly, *Journal of Power Sources*, 109 (2002) 356-364.
9. P. Costamagna, C. Yang, A. B. Bocarsly and S. Srinivasan, *Electrochimica Acta*, 47 (2002) 1023-1033.
10. C. Yang, S. Srinivasan, A. B. Bocarsly, S. Tulyani and J. B. Benziger, *Journal of Membrane Science*, 237 (2004) 145-161.
11. W. Mérida, University of Victoria, *Thesis Doctor of Philosophy*, 2002
12. Z.-G. Shao, P. Joghee and I. M. Hsing, *Journal of Membrane Science*, 229 (2004) 43-51.
13. A. Sacca, I. G. A. Carbone, R. Pedicini and E. Passalacqua, *Journal of Power Sources*, 163 (2006) 47.
14. S. J. Park, D. H. Lee and Y. S. Kang, *Journal of Membrane Science*, 357 (2010) 1 - 5.
15. J. Wu, Z. Cui, C. Zhao, H. Li, Y. Zhanga, T. Fu, H. Na and W. Xing, *International Journal of Hydrogen Energy*, 34 (2009) 6740 - 6748.
16. S. K. Seshadri, H. M. Alsyouri and Y. S. Lin, *Microporous and Mesoporous Materials*, 129 (2010) 228 - 237.
17. A. Alvarez, C. Guzmán, A. Carbone, A. Saccà, I. Gatto, R. Pedicini, E. Passalacqua, R. Nava, R. Ornelas, J. Ledesma-García and L. G. Arriaga, *Journal of Power Sources*, 196 (2011) 5394–5401.
18. A.S. Arico, P. Creti, P. L. Antonucci and V. Antonucci, *Electrochemical and Solid-State Letters*, 1 (1998) 66-68.
19. T. Romero and W. Mérida, *Journal of Membrane Science*, 338 (2009) 135-144.
20. A. Alvarez, C. Guzmán, A. Carbone, A. Saccà, I. Gatto, E. Passalacqua, R. Nava, R. Ornelas, J. Ledesma-García and L. G. Arriaga, *International Journal of Hydrogen Energy*, (2011) Submitted.
21. C. Guzmán, A. Alvarez, O. E. Herrera, R. Nava, J. Ledesma-García, L. A. Godínez, L. G. Arriaga and W. Mérida, *International Journal of Electrochemical Science*, 6 (2011) In press.
22. V. Antonucci, A. Di Blasi, V. Baglio, R. Ornelas, F. Matteucci, J. Ledesma-García, L. G. Arriaga and A. S. Arico, *Electrochimica Acta*, 53 (2008) 7350-7356.
23. A.S. Arico, V. Baglio, A. Di Blasi, P. Creti, P. L. Antonucci and V. Antonucci, *Solid State Ionics*, 161 (2003) 251-265.